Journal of Atmospheric and Solar-Terrestrial Physics 173 (2018) 109–118

Contents lists available at ScienceDirect

Journal of Atmospheric and Solar-Terrestrial Physics

journal homepage: www.elsevier.com/locate/jastp

Rain characterization based on maritime and continental origin at a tropical location

Saurabh Das *, Chandrani Chatterjee

Center for Soft Computing Research, Indian Statistical Institute, 203 Barrackpore Trunk Road, Kolkata, 700108, WB, India

ARTICLE INFO

Keywords:
Drop size distribution
Maritime and continental precipitation
Quantitative precipitation estimation
Z-R relation
Rain attenuation

ABSTRACT

Quantitative precipitation estimations (QPE) from remote sensing observations requires understanding of the rain characteristics. Rain drop size distribution (DSD) is the fundamental parameter for characterizing rain and depends strongly on the climate, origin and precipitation type. Past studies are mostly concentrated on the DSD variations on locations and rain type, but only a few studies focused on the rain DSD difference between maritime and continental circulation. The aim of the present study is to analyse the different precipitation properties associated with maritime and continental rain at a coastal Indian location. The rain rate probability, DSD parameters, rain rate(R)-radar reflectivity (Z) relation and rain attenuation under different rain conditions are presented here based on three years of DSD measurements at Trivandrum (08°52′, 76°93′). Higher value of mean rain rate is observed for maritime rain than continental rain. The Z-R relation is also found to be significantly different for these two types of rain. Abundance of smaller drops is indicated in maritime rain whereas large raindrops has dominance in continental rain. The rain attenuation associated with maritime rain also found to be notably higher than the continental rain. The coefficients for converting the rain rate to attenuation values for different frequencies are estimated for the present location. The results indicate the scope of improvement in QPE by adjusting the Z-R relation from the characteristics difference in rain microstructure/attenuation for continental and maritime rain.

1. Introduction

Precipitation has been on the top of climatic items of interest since eras. The advancement of remote sensing techniques and satellite-borne radars provide a great tool to study the precipitation throughout the globe in real time fashion (Tian et al., 2007; Adler et al., 2009; Islam et al., 2012a,b). However, the estimation of rainfall amount from remote sensing observations need better quantifications of the rain-signal interaction and knowledge of rain micro-physics (Delgado et al., 2008; Ojo and Omotosho, 2013; Das and Maitra, 2016). Characterising the same in all possible aspect, however, remains a challenging job due to limited experimental measurements and wide variability of rain features (Lee and Zawadzki, 2005; Nesbitt et al., 2006; Tapiador et al., 2010).

The precipitation is normally characterized by drop size distribution (DSD). The rain intensity and other rain integral parameters can be studied with the knowledge of DSD (Joss and Waldvogel, 1969; Bringi and Chandrasekar, 2001). However, there does not exist any unique model of DSD which can represent all types of rain and for different geographic locations (Timothy et al., 2002; Das et al., 2010; Das and Maitra, 2017). The variability of rain characteristics arises due to the differences in DSDs. Since the rain drops are the source of signal interaction, hence, the varied DSD affect the accuracy of quantitative precipitation estimation (QPE). The rain attenuation and radar reflectivity (Z)-rain rate(R) relation varies due to the same reason and are sources of major uncertainty in QPE. Several studies on this area has been done in the past (Morin and Gabella, 2007; van De Beek et al., 2016; Das and Ghosh, 2016; Montopoli et al., 2017) but the answer remains incomplete due to limited understanding of DSD variations for different locations and reasons.

DSD has known dependency on the rain types (stratiform/convective), geography (tropical/temperate), orography and rain rate (Sauvageot and Lacaux, 1995; Harikumar et al., 2010; Thurai et al., 2016). The Z-R relation and radar reflectivity-specific rain attenuation (γ) relations are studied by different researchers for improvement in QPE in different rain conditions. However, the majority of past studies are mostly concentrated on the temperate regions (Atlas and Ulbrich, 1977; Wilson and Brandes, 1979; Ulbrich and Lee, 1999; Thurai et al., 2016) and data from tropical regions are still scattered (Das and Maitra, 2016). Since, it's

* Corresponding author.
E-mail addresses: saurabh_t@isical.ac.in, das.saurabh01@gmail.com (S. Das), chandrani.chatterjee9@gmail.com (C. Chatterjee).

https://doi.org/10.1016/j.jastp.2018.02.011
Received 10 August 2017; Received in revised form 2 January 2018; Accepted 25 February 2018
Available online 6 March 2018

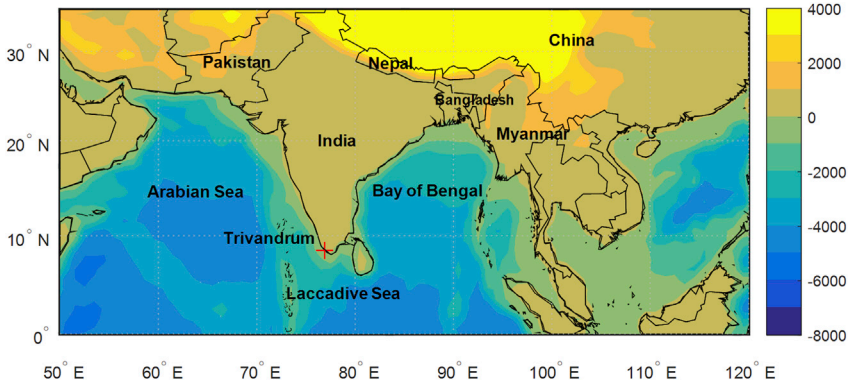

Fig. 1. Geographic location of the experimental site. The colour bar indicates the topographic height in meter.

not always possible to discriminate the rain in stratiform and convective types for real time applications, the analysis of the DSD variations for different wind circulations, particularly for maritime and continental wind, can provide useful information for improvement in QPE.

There are characteristic differences between land generated precipitation and sea generated ones. Various studies have also reported that the difference between maritime and continental rain is not uniform all over the world and it depends on coast shape and topographical characteristics of the region (Zipser et al., 2006). As the land and sea aerosol are different, therefore, the drop size spectra of maritime and continental cloud formation is also different. Large difference between maritime and continental convective clouds was reported earlier (Rosenfeld and Lensky, 1998). They observed significant transformations in the microphysical and precipitation forming processes of convective clouds moving from sea towards land. Yum and Hudson (2002) observed substantial distinction between maritime and continental cloud microphysics related to cloud condensation nuclei (CCN) concentration based on 15 h of in-situ cloud measurements in Atlanta and Pacific stratus. The study considered thin stratus clouds and reported two times greater liquid water content in maritime clouds than continental. They showed significant greater light rain water content in maritime precipitation than in continental rain. The distinction reported by them was further supported by Göke et al. (2007). They investigated X-band RADAR reflectivity evolution of cloud using the entire summertime small cumulous microphysical study (SCMS) dataset of Floridian north-eastern coast. A method of identifying maritime and continental clouds with radar data was further proposed by the authors. Tenório et al. (2012) studied a DSD data set collected at a coastal site in North-Eastern Brazil to examine the difference between rainfall parameters associated with maritime and continental precipitation. They noted significant higher mean rain rate for maritime rain than continental rain. They also observed an opposite behaviour of maritime and continental DSD. A significant difference in rainfall parameters for precipitation generated due to maritime and continental clouds were observed in their study and emphasized on the requirement of using distinct coefficients of *Z-R* relationship for estimating rain in such situation. However, most of the past studies mostly focused on the cloud characteristics, and not much on rain characteristics.

There were several studies on rain characteristics of tropics, particularly over Southern India in past. South India receives a substantial rainfall due to its geographic location near the equator. Rao et al. (2009, 2001) observed significant differences between DSD of north-eastern (NE) and south-western (SW) monsoon at a south Indian location Gadanki. The study reported redundancy of smaller drops in NE monsoon. The wind field and rain parameters studied by them implied continental and maritime nature respectively in SW and NE monsoon. Rain drop size distribution before and after landfall of three cyclones were studied by Janapati et al. (2017) using disdrometer in two different locations (Gadanki and Kadpa) in south India. Higher mass weighted mean diameter and lower normalized intercept parameter values are

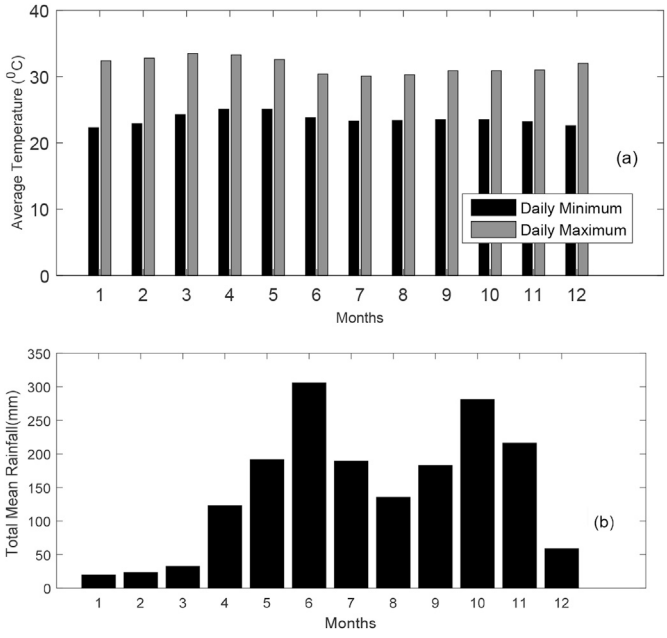

Fig. 2. Annual variation of (a) temperature and (b) rainfall amount at Trivandrum.

reported in convective precipitation than in stratiform rainfall. The *Z-R* relation reported to have notable distinction for the two cases. Das and Maitra (2017) studied the DSD characteristics of different locations in India. They have reported the variations of DSD characteristics and associated rain parameters for different rain types including stratiform and convective rain. The rain attenuation features and *Z-R* relations are also studied based on the DSD measurements. However, little attempt has been made to study the characteristics difference between continental and maritime rain over Indian region. The aim of the present study is to examine the characteristics of maritime and continental rain at Trivandrum, a tropical region in southern India. The data has been collected during 2005–2007 using an impact type Disdrometer.

2. Data and methodology

2.1. Experimental details

The DSD measurement is performed by an impact type (Disdromet, RD 80) disdrometer at Trivandrum under ISRO's Ka band propagation experiment. Trivandrum is situated at the west coast in Southern India as indicated in Fig. 1. The city is bounded by ocean to its west and the Western Ghat mountain range to its east. The average elevation of the city is about 16 feet from the sea level. It is quite interesting to study the

precipitation characteristics of this city as it borders between the Tropical Savanna Climate and the Tropical Monsoon Climate (Chandra et al., 2016). The average annual rainfall in Trivandrum is about 1800 mm. The city gets majority of its rainfall due to south-west monsoon during June–September, but the receding north -eastern monsoon also causes substantial rain during the month of October–November. Fig. 2 shows the annual temperature and precipitation variation of the location based on 10 years data.

The disdrometer fundamentally measures the rain drop size distribution and rest of the rain parameters are calculated based on DSD. It is an impact type drop size counter which can sense drops within a range of 0.3mm–5 mm diameter with an accuracy of ± 5% and distinguishes 127 classes of drop diameters. The momentum of the drops are basically measured by the disdrometer. The drop size diameter is then calculated from the fall velocity with a presumption that the drops are falling with their terminal velocity (Gunn and Kinzer, 1949). For the practicality of calculation and for getting statistically meaningful samples, the 127 drop sizes are combined into 20 drop size classes distributed more or less exponentially over the available range of diameter drop.

There are some known issues with this type of disdrometer measurements, such as dead time. This disdrometer underestimates small drops while responding to a bigger drop, known as dead time. The accuracy is also degraded under windy conditions due to acoustic noise. In spite of these facts, it is one of the widely used and tested instrument for its stability and performance (Ulbrich, 1983; Feingold and Levin, 1986; McFarquhar et al., 1996; Das and Maitra, 2016).

The disdrometer was operated at 30s temporal resolution. Since the catchment area of the instrument is small (~50 cm^2), the small integration time is always not sufficient to get the actual DSD (Islam et al., 2012a,b). This is particularly true for large drops during heavy rains. The small drops are also underestimated in JW disdrometer in comparison with optical or radar measurements (Sarkar et al., 2015). However, the small drops have less effect on estimating the rain integral parameters from DSD. The underestimation of large drops are found to be significant above 20 mm/h rainfall (Sarkar et al., 2015).

Though large integration time of disdrometer can lead to better individual DSD estimation, the effect of integration time is found to be less when long term average DSD is studied. Asen and Gibbins (2002) showed the effect of integration time on the long term average of DSD with two disdrometer data sets of Chilbolton (10s resolution) and Singapore (30s resolution). The Singapore data shows smaller spread than Chilbolton data around the mean due to increase in integration time in first case. However, they also reported that the standard deviation around the long term mean become very small with increase in the number of samples. Maitra et al. (2009) compared the rain rate estimated from disdrometer measurements of 30s resolution at Ahmedabad with that of collocated tipping bucket rain gauge measurements with reasonable agreement. The rain rate and DSD estimated from disdrometer with 30s integration time is also compared with Micro Rain Radar derived DSD and rain rate at 200 m height at Ahmedabad (Das et al., 2010, 2016). The results are in close agreement with each other, though some underestimation of drops can be noted. The average DSD characteristics at different Indian locations for different types of rain are also studied by Das and Maitra (2016, 2017) with same 30s integration time.

2.2. Methodology of data analysis

To identify the maritime and continental circulation, 5-days back trajectory analysis has been done. The advantage of back-trajectory analysis over the radar measurement, which also shows the motion of precipitating system, is that one can identify the movement of wind for sufficiently long time backward. For back trajectory calculation, Trajstat software (Wang et al., 2009) has been used. Trajstat is a GIS based software plugin of MeteoInfo (http://www.meteothinker.com/index.html). The trajectory calculation function of Trajstat is governed by the Hybrid Single-Particle Lagrangian Integrated Trajectory (HYSPLIT) Model developed by NOAA (https://ready.arl.noaa.gov/HYSPLIT.php). Here, the flow field of air (reaching a location) in space and time is given by the backward trajectory of an air parcel. Lagrangian framework is adopted for the identification of water vapour source related to rainfall. HYSPLIT uses gridded four-dimensional (x, y, z, t) meteorological fields output as analysis or forecast fields from the NOAA NCEP weather prediction models. HYSPLIT model (Draxler and Hess, 1998) is extensively used for trajectory analysis in several studies. For e.g., Deshpande et al. (2015) demonstrates successful identification of the water vapour source of 93.3% rain bearing winds in Ahmedabad as Arabian Sea (AS), Bay of Bengal (BoB) or recycled using back trajectory analysis. Purdie et al. (2010) identified the moisture source region in Alps using HYSPLIT model effectively for studying the elemental changes in winter snow.

Table 1
Details of the experimental data.

Total number of days with available data	609
Number of days with no rain	26
Number of rainy days with ambiguous wind flow direction	27
Number of rainy days with maritime wind	519
Number of rainy days with continental wind	37

For the present study, the back trajectory analysis has been done over Trivandrum for all rainy days of 2005–2007 at a height of 2000m. The long distance pathways of water vapour responsible for each rain event are then traced using HYSPLIT model. Rain in Trivandrum is influenced either by the wind containing moisture pick up from AS and BoB or it can be generated over the Indian landmass. While drawing the trajectories, the process of air compression was assumed to be isentropic in nature. For the present analysis, we choose only those dates where the back trajectories were either fully over the land surface or over the oceans. We excluded the dates where some part of back-trajectory is over land or sea. With this strict criterion, we are able to separate 519 days of maritime and 37 days of continental rain as mentioned in Table 1. A typical example of 5-days back-trajectories are shown in Fig. 3(a) and (b) for maritime and continental wind for the month of October 2007, respectively. The example of ambiguous back-trajectory is shown in Fig. 3 (c).

Different precipitation parameters like rain rate, drop size distribution, radar reflectivity and rain attenuation are then investigated in order to understand the characteristic differences between rain occurring from maritime and continental precipitating system. To compare the DSD, the number concentration of drops is further modelled in the lognormal function as (Timothy et al., 2002)

$$N(D) = \left(\frac{N_T}{\sigma D\sqrt{2\pi}}\right)\exp\left[-\frac{0.5(lnD-\mu)^2}{2\sigma^2}\right] \quad (1)$$

Where $N(D)$ is the number density of rain drops (in $m^{-3}mm^{-1}$), N_T is the total number of rain drops, D is the rain drop diameter (in mm), μ and σ are the mean and standard deviation of $ln\ (D)$.

In the present study, the lognormal model is preferred over gamma model, which is another popular function of modelling DSD, because DSD parameters used in this model have very clear physical meaning. Method of Moments technique is used here for computing the three basic parameters of lognormal model N_T, μ and σ because of its linear relation with the moments of DSD and the 3rd, 4th and 6th moments are considered for estimating the DSD parameters as follows (Kozu and Nakamura, 1991):

$$N_T = \exp\left[\frac{1}{3}\left(24L_3 - 27L_4 + 6L_6\right)\right] \quad (2)$$

$$\mu = \frac{1}{3}\left(-10L_3 + 13.5L_4 - 3.5L_6\right) \quad (3)$$

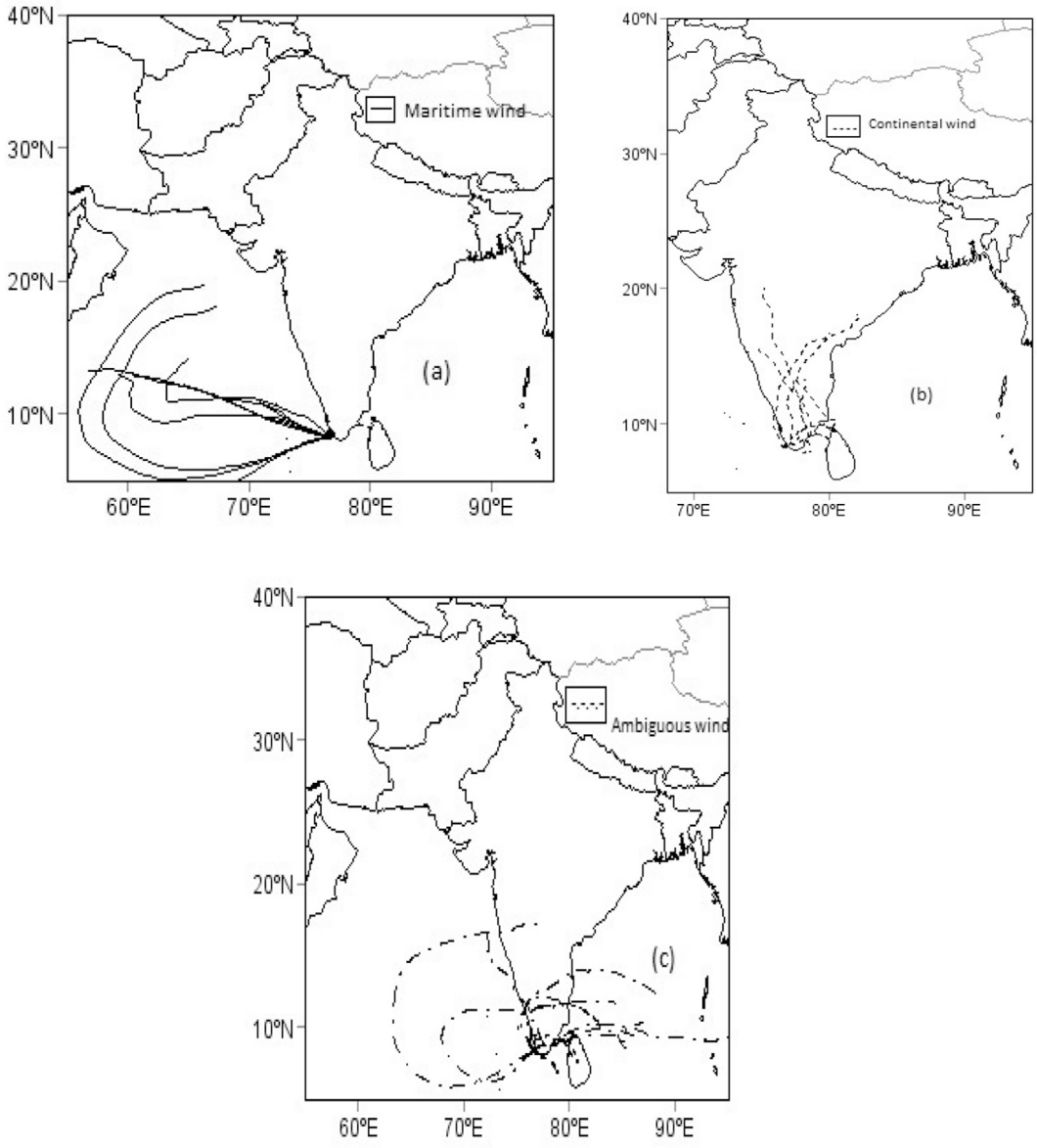

Fig. 3. Back trajectory of wind regenerated by Trajstat. Days with (a) maritime, (b) continental and (c) ambiguous wind direction during October 2007.

$$\sigma^2 = \frac{1}{3}(2L_3 - 3L_4 + L_6) \tag{4}$$

Where, L_3, L_4 and L_6 are the natural logarithms of 3rd, 4th and 6th moments respectively.

The rain integral parameters such as, rain rate, radar reflectivity and rain attenuation can now be estimated based on the DSD as follows (Joss and Waldvogel, 1969; Doviak and Zrnić, 1984, 184–194; V N Bringi and Chandrasekar, 2001):

$$R = \frac{\pi}{6} * \frac{3.6}{1000} * \frac{1}{At} \sum_{i=1}^{20} (n_i D_i^3) \tag{5}$$

$$Z = \frac{1}{At} \sum_{i=1}^{20} \frac{n_i}{V(D_i)} * D^6 \tag{6}$$

$$\gamma\left(\frac{dB}{km}\right) = 4.343\ X\ 10^{-3} \int_0^{\alpha} Q_t(D) N(D) dD \tag{7}$$

Where, A represents total area of observation, t denotes time interval between observations, n_i denotes total number of drops in i^{th} drop size class, D_i represents mean diameter of i^{th} drop size class and $V(D_i)$ is the fall velocity of a rain drop having diameter D_i. Q_t is the attenuation cross-section of rain drops expressed in units of area. Attenuation cross section is a function of the drop radius, wavelength of the radio wave and complex refractive index of the water drop and is calculated using Mie scattering theory (Ippolito, 1986).

The attenuation cross section Q_t (in mm^2) is given by (Yeo et al., 2001).

$$Q_t = \lambda^2 / 2\pi \sum_{n=1}^{\alpha} (2n+1) Re[a_n + b_n] \tag{8}$$

where, a_n and b_n are the Mie scattering coefficients, which are complex functions of drop diameter, wavelength and complex refractive index of water respectively, and Re denotes the real part (Ippolito, 1986). As the complex refractive index of water depends on the temperature, the Q_t also depends upon the temperature.

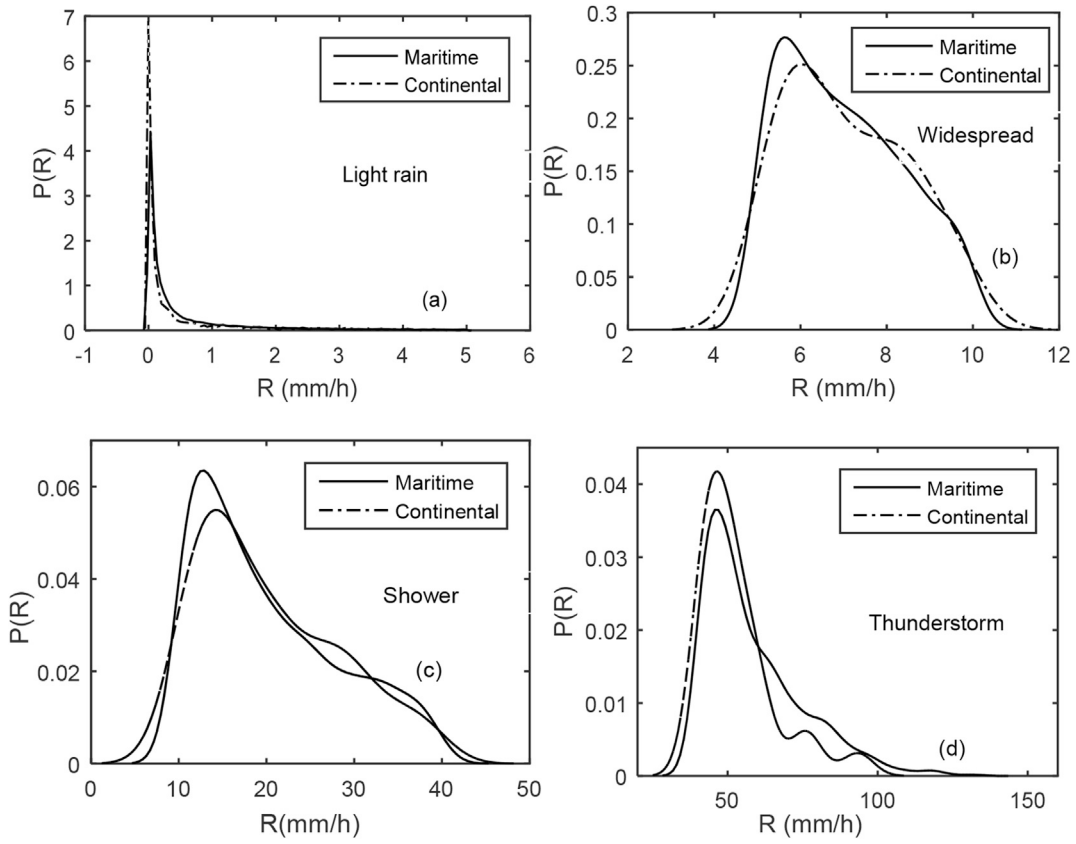

Fig. 4. Probability density function of rain rate for maritime and continental rain.

Table 2
Statistical parameters for the probability density function of rain rate.

	Maritime				Continental			
	Mean	Variance	Kurtosis	Skewness	Mean	Variance	Kurtosis	Skewness
R < 5 mm/h (Drizzle)	0.58	0.95	8.72	2.45	0.49	0.89	9.08	2.54
5 < R < 10 mm/h (Widespread)	7.01	1.96	2.06	0.40	7.09	1.95	1.93	0.37
10 < R < 40 mm/h (Shower)	20.10	66.09	2.41	0.72	20.32	63.41	2.40	0.68
R > 40 mm/h (Thunderstorms)	58.36	269.42	4.58	1.32	52.99	165.11	5.38	1.64

The DSD characteristics have been studied for different rain rate ranges as DSD varies with rain rate. The data set is categorized in following four rain rate ranges, 0–5 mm/h (light rain), 5–10 mm/h (widespread), 10–40 mm/h (shower) and >40 mm/h (thunderstorm). The rain attenuation has also been studied for different frequencies in the range 10–100 GHz and for these rain rate classes for similar reason.

3. Results and discussions

3.1. Rain rate characteristics

The probability distribution of rain rate for maritime and continental rain are shown in Fig. 4(a–d). The probability density function (PDF) of rain rate < 5 mm/h is almost similar for both types of rain. The PDFs of rain rate ($R > 5$ mm/h) for both the rain subsets, however, resemble lognormal distributions. Both the rain rate distributions are leptokurtic and positively skewed though the peak is shifted towards left (except light rain) for maritime rain indicating the dominance of lower intensity rain. This also implies more frequent occurrence of stratiform type in maritime rain than in continental rain since low rain rate are normally associated with stratiform rain. The statistical parameters of the probability distributions are summarized in Table 2.

3.2. DSD characteristics

As already mentioned, to study the DSD characteristics, the individual DSD has been modelled in log-normal form. The model parameters μ, σ and N_T are then modelled in terms of rain rate. The modelled log-normal parameters for this study area representing average maritime and continental rain characteristics are given in Table 3. It is evident that the model parameters are notably different for maritime and continental rain types. Particularly, the total rain drop number, N_T, is significantly high for maritime rain.

To study the change in characteristics of these rain types for different rain rates, the data sets are further divided in four rain rate classes as mentioned in the earlier section. The average DSD of maritime and continental rain for four different rain rate classes are shown in

Table 3
Modelled Log-Normal parameters.

	N_T	μ	σ^2
Maritime	$161.09\ R^{0.47}$	$-0.1558 + 0.1219 \ln(R)$	$0.0616 + 0.008423 \ln (R)$
Continental	$92.38\ R^{0.49}$	$-0.0261 + .1153 \ln (R)$	$0.07 + 0.00088 \ln (R)$

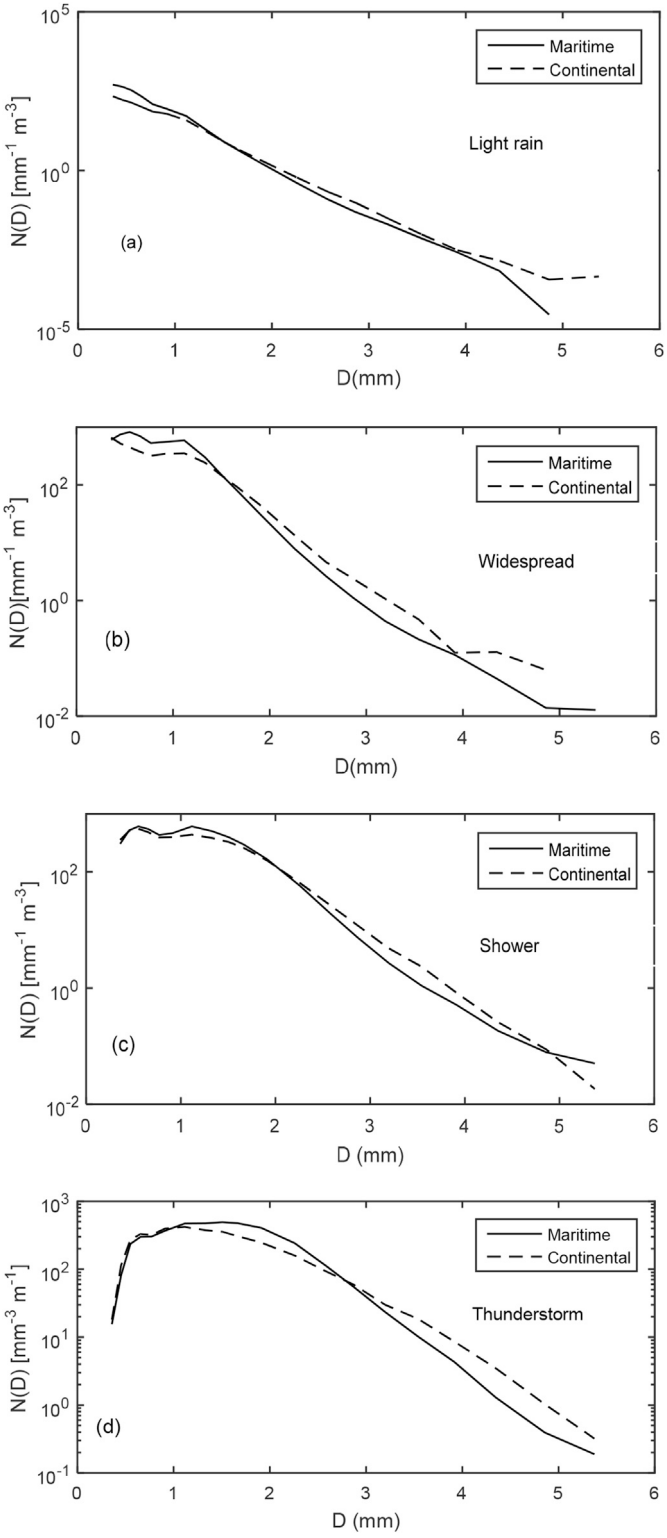

Fig. 5. The averaged number concentration with drop diameter over four rain-rate classes.

Fig. 5(a–d). The DSD for maritime and continental rain seem to have distinguishable behaviour in each of the rain rate classes considered. The number concentration for maritime rain is higher than continental rain for small drop size diameter in all the classes. In contrast, for large rain drops, the number concentration of continental rain dominates over maritime rain. Similar observations are also reported by several researchers for maritime and continental rain (Tokay et al., 2002; Rosenfeld and Ulbrich, 2003; Bringi et al., 2003; Ulbrich and Atlas, 2007). This again indicates dominance of smaller drops in maritime rain in comparison with continental precipitation. There exist a critical diameter where this behaviour of number concentration toggled. However, this critical diameter is not constant for all the rain rate classes and varies in the range 1.5–3 mm. The critical diameter shifts towards larger drops with increasing rain intensity.

Fig. 6 shows the probability distribution of mean volume diameter in four different rain rate classes. The mean volume diameter is estimated from the ratio of forth and third moment of DSD (Das and Maitra, 2016). The probability density functions of mean volume diameter for maritime and continental precipitation are similar in nature and represent normal distributions. The peak of the distribution, however, found to shift towards large values with increasing rain intensity for both the cases. Interestingly, there are secondary peaks in higher rain rate classes for continental rain which are not present in case of maritime rain. Those secondary peaks are towards large drop diameter values. This again indicates dominance of large rain drops in continental rain.

Table 4 summarizes the statistical description of the variation of mean volume diameter. It is also been used as an indicator to get an idea about the variability of rain DSDs in a particular rain rate range. It can be noticed that in case of maritime rain, the magnitude of the peaks increase with increase in rain rate (except widespread rain) and reverse scenario is observed in case of continental rain (except light rain). The quartile deviation for the two distribution have been calculated for each rain rate class for getting a clearer view of the measure of spread. The variation of DSD in continental rain is found to be more than maritime rain. In maritime rain, the quartile deviation has increased with increasing rain rate (except light rain) whereas, for the continental rain the quartile deviation has shown a decreasing trend with increase in rain rate (except thunderstorm). The position of the peak in the distribution of mean volume diameter is always higher in case of continental rain than maritime rain similar to the observations from other regions (Tokay et al., 2002; Rosenfeld and Ulbrich, 2003; Bringi et al., 2003; Ulbrich and Atlas, 2007). In case of Trivandrum, the mean volume diameter for maritime rain varies in the range of 1.56–2.01 mm for $R > 10$ mm/h, while in case of continental rain it varies in the range of 1.7–2.2 mm. In a similar observation Rao et al. (2009) obtained mean volume diameter varies between 1.5 and 2.6 mm for SW monsoon and between 1.3 and 2.2 mm for NE monsoon over Gadanki, a location along east coast of Southern peninsular India. They confirmed from wind direction observation that the NE monsoon over Gadanki is Oceanic whereas SW monsoon is continental type and the continental rain are having more large drops than oceanic rain.

3.3. Z-R relationship

Improvement in radar estimation of rainfall rely mostly on the proper modelling of the *Z-R* relation. Various studies have documented that *Z-R* relation can vary geographically, with precipitation types and even for rain events (Kumar et al., 2011; Raghavan, 2013; Das and Ghosh, 2016; Das and Maitra, 2016). Therefore, it is interesting to study the differences in the values of power law coefficients for maritime and continental rain in Indian context. Empirical expression of the form $Z = aR^b$ usually describes the relationship between these two parameters. For the present study, the parameters are estimated using linear regression technique between ln (Z) and ln(R). For maritime rain, the regression coefficients a and b are found to be 191.71 and 1.352, respectively with a coefficient of determination (R^2) of 0.96. In case of continental rain, the coefficient a and b are found to be 279.78 and 1.34, respectively with the coefficient of determination (R^2) of 0.97. Usually, a high a value indicates convective rain type for the present location (Das and Maitra, 2016). The improvement in QPE is thus possible with proper choice of *Z-R* relation depending upon the maritime/continental origin of rain.

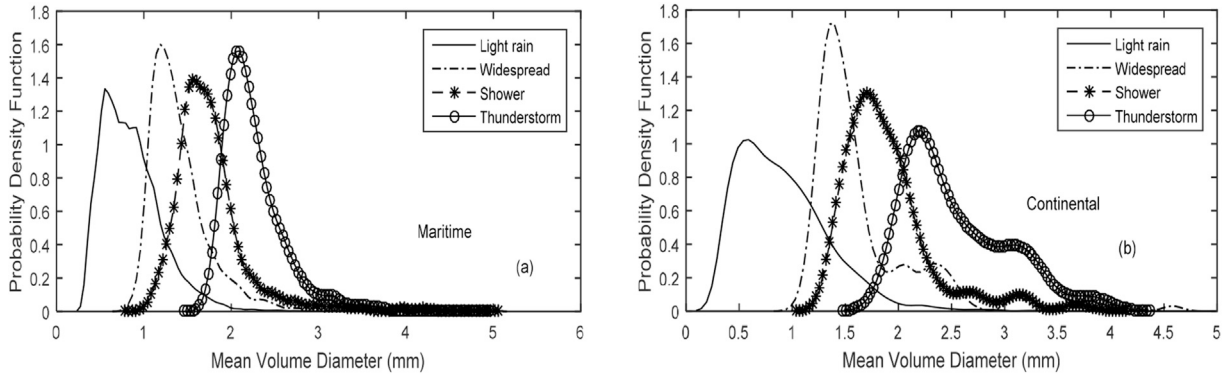

Fig. 6. Probability density function of mean volume diameter for (a) maritime and (b) continental precipitation for different rain rate classes.

Table 4
Statistical properties of the probability density function of mean volume diameter for maritime and continental rain.

	Peak Position (in mm)		Kurtosis		Quartile deviation	
	Maritime	Continental	Maritime	Continental	Maritime	Continental
R < 5 mm/h (Light rain)	0.55	0.59	7.457	8.172	0.23	0.291
5 < R < 10 mm/h (Widespread)	1.18	1.40	14.455	9.978	0.191	0.225
10 < R < 40 mm/h (Shower)	1.56	1.70	12.778	7.349	0.193	0.203
R > 40 mm/h (Thunderstorms)	2.09	2.21	10.158	3.008	0.194	0.344

Table 5
Coefficients of specific attenuation calculated over different frequencies.

Frequency (GHz)	Maritime		Continental		ITU-R	
	k	*α*	*k*	*α*	*K*	*α*
10	0.0075	1.0592	0.0084	1.10537	0.0117	1.2371
20	0.0587	1.1239	0.0672	1.1067	0.0938	1.0198
30	0.1531	1.0937	0.1663	1.0812	0.2347	0.9311
40	0.2792	1.0656	0.2928	1.0570	0.4352	0.8549
50	0.4290	1.0365	0.4332	1.0308	0.6536	0.7978
60	0.5891	1.0032	0.5704	1.0014	0.8560	0.7571
70	0.7431	0.9670	0.6907	0.9701	1.0284	0.7280
80	0.8775	0.9301	0.7870	0.9386	1.1686	0.7068
90	0.9876	0.8948	0.8592	0.9084	1.2801	0.6910
100	1.0755	0.8628	0.9119	0.8806	1.3675	0.6789

3.4. Rain attenuation

Radar frequencies above 10 GHz are very sensitive for studying precipitation. Increasing the frequency provides better detailing of cloud microphysics and precipitation forming processes. The precipitation monitoring satellites like TRMM (Tropical Rainfall Monitoring Mission) and GPM (Global Precipitation Measurement) are using high frequency radars. GPM is equipped with Dual Precipitation Radar (working at 13.6 GHz and 35.5 GHz) for studying the rain microphysics to a greater

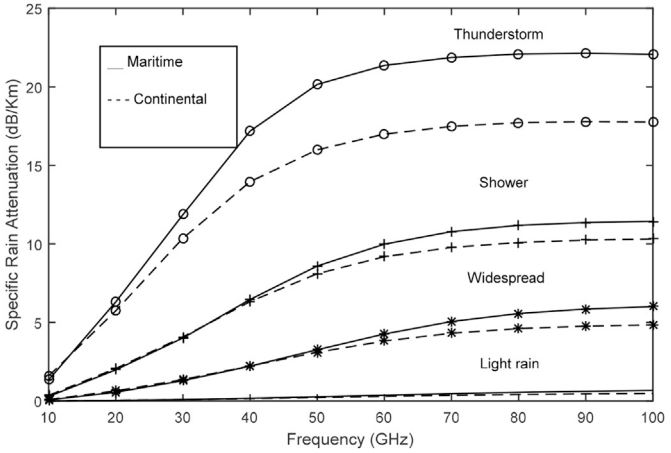

Fig. 8. Variation of specific attenuation with frequencies for maritime and continental rain.

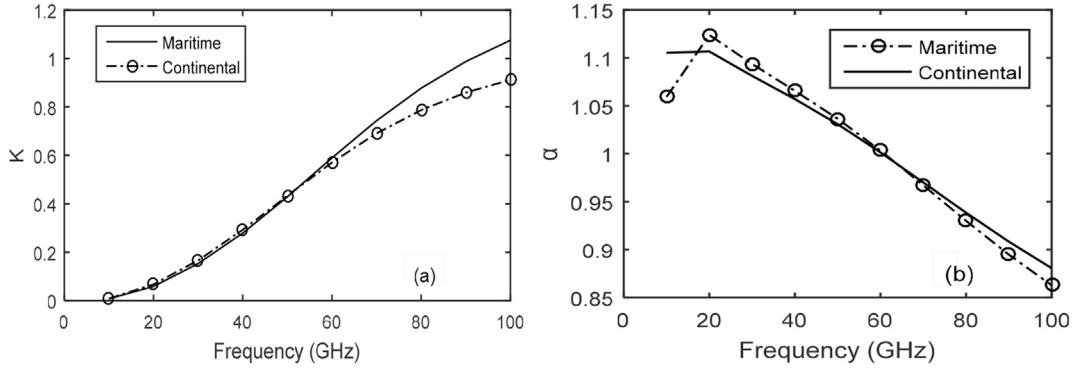

Fig. 7. Behaviour of coefficients of specific rain attenuation (a) k and (b) α for maritime and continental rain.

accuracy over single band (13.6 GHz) TRMM. On the other hand, the rapid advancement in radio communication in recent days is creating the need of higher frequency bands to be used. However, rain also attenuates signals which increases with increase in rain rates and frequencies. Hence, estimation and compensation of rain attenuation become important for high frequency radars and communication systems (Moupfouma, 1984).

The probable rain attenuation is studied using the measured DSD for these two types of rain and for different frequencies. The power law coefficients of the empirical formula, $\gamma = kR^{\alpha}$, are determined at 10 different frequencies in the range 10–100 GHz. The coefficients calculated by the linear regression analysis are shown in Table 5. The values are compared with the ITU-R model (ITU R P838-3, 2005) which is normally used as reference for such purposes. It is observed that the coefficients k for continental rain are larger than that of maritime rain for frequencies up to 60 GHz whereas it reversed for frequencies above 60 GHz (Fig. 7). The behaviour of coefficient α is mostly opposite to the behaviour of k.

In Fig. 8, the specific attenuation for maritime and continental rain are shown for different rain rates and frequencies. The specific attenuation depends on the temperature and for the present study, it is assumed to be 303 K. Since Trivandrum is situated in a coastal region, the diurnal or seasonal variations are limited. Hence, average specific attenuation of maritime and continental rain will have limited dependence on the temperature.

The difference between maritime and continental rain is very prominent for all types of rain. The specific rain attenuation in maritime rain is always higher than continental rain and the difference between specific attenuation in maritime and continental rain increases with increase in rain intensity. The results strongly indicate the need of separate rain attenuation correction model for maritime and continental rain. It also indicates that the rain attenuation information can be a good indicator to separate the maritime and continental rainfall.

4. Monsoon effect on the study

As already pointed out, rain DSD depends on many factors and monsoon circulation is one of the important factors for Trivandrum. Trivandrum receives substantial rainfall during both SW and NE monsoon. The wind direction at this location during SW monsoon is mostly from the sea whereas wind flows from landmass during NE monsoon. The DSD and associated rain characteristics described above are based on overall events which essentially include samples from both type of monsoons. There are several studies highlight contrasting effects of these two types of monsoon (Rao et al., 2001; Kozu et al., 2006). However, the exact reason for such change in characteristics is yet to be ascertained. Kirankumar et al. (2008) studied the vertical profile of rain DSD from VHF and UHF radar at Gadanki, another location is southern peninsular India and compared the continental monsoon rain with results obtained at Durwin, Australia having Oceanic monsoon regime. They obtained similar vertical structure during stratiform rain, however, obtained a different vertical structure of mean volume diameter during convective phase. The monsoon dependence of the DSD characteristics, particularly the changes in gamma model parameters, over Trivandrum are also investigated by Das and Maitra (2017). As pointed by Das and Maitra (2017), though the average DSD characteristics changes for NE and SW monsoon, the microphysical characters are mostly remain same for stratiform and convective cases irrespective of monsoon circulation. These previous studies raise an important question whether the change in average DSD characteristics is due to change in monsoon circulation or due to origin of the cloud system from sea or land surfaces. Rao et al. (2009) investigate in depth the DSD characteristics changes during NE and SW monsoon at Gadanki to answer this question. They discussed several possible pathways in cloud formation process and in rain evolution phase as responsible for such contrasting effect. The oceanic and continental flow of the monsoon winds are identified as one of the primary reason for such change during cloud formation process at Gadanki.

In the present study, the back-trajectory analysis ensures that the air mass parcel is over land or sea for a sufficiently long time before reaching the study location and the rain is categorized based on that. To further ascertain whether the observed change in maritime/continental rain is simply because of monsoon circulation or not, we have repeated the above study excluding the monsoon months (i.e., excluding June–Sept. for SW monsoon and Oct.–Nov. for NE monsoon). In Fig. 9, the characteristics of maritime and continental rain for light rain are shown for non-monsoon months as an example. It can, still, be observed that the maritime and continental rain have distinct characteristics and are in agreement with earlier discussed results.

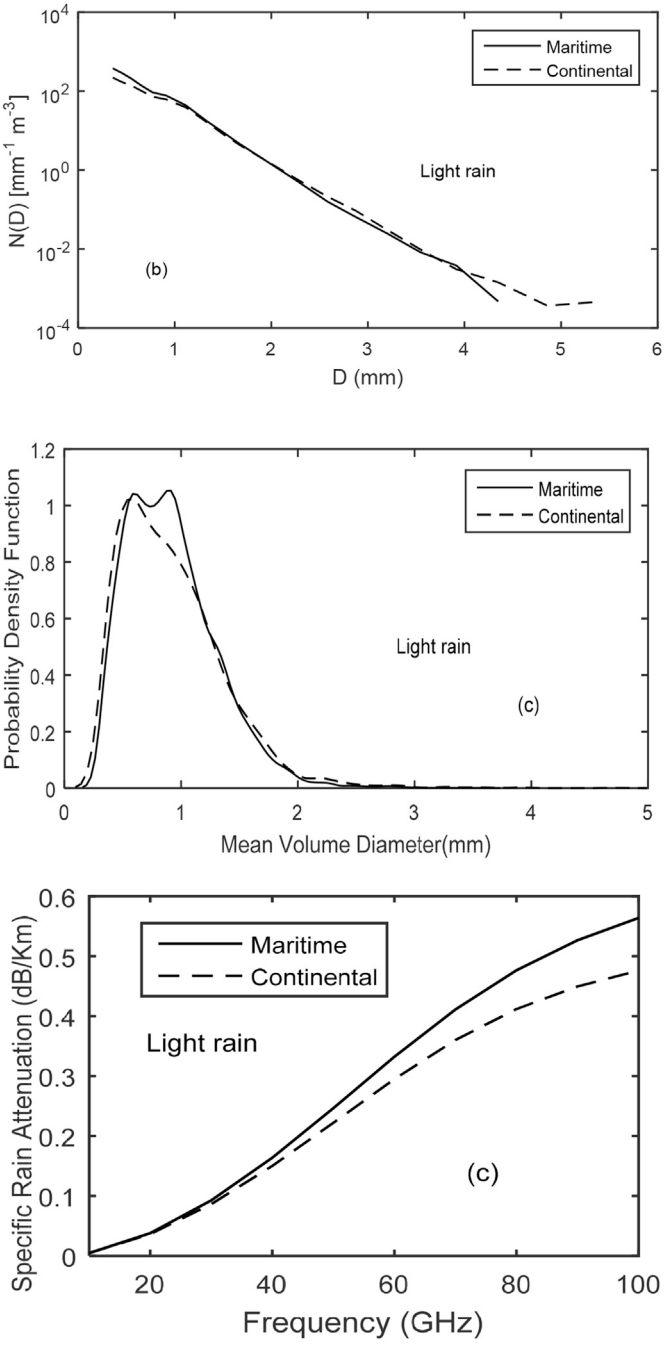

Fig. 9. Rain features of Nonmonsoon maritime and continental rain. (a) The averaged number concentration with drop diameter, (b) Probability density function of mean volume diameter and (c) Variation of specific attenuation with frequencies for maritime and continental rain.

5. Conclusion

In this paper, rain characterization and its effect on signal propagation have been studied for maritime and continental rainfall at a tropical location in India. Maritime and continental precipitation showed prominently visible characteristic differences. The rain rate distribution shows more low intensity rain in maritime rainfall than in continental rainfall. The modelled DSD parameters clearly show that maritime and continental rain needed to be considered separately as there are notable difference in the values of rain features for these two types of rain. The nature of DSD for maritime rain showed contrasting behaviour with that of continental precipitation. The total number of rain drops in maritime rain is almost twice than that of continental rain. Abundance of smaller drops is observed in maritime rain whereas large raindrops has dominance in continental rain. This is also supported by the probability distribution of mean volume diameter. The *Z-R* relation for maritime and continental precipitation at Trivandrum has also been estimated. The results indicate that the stratiform rain events are frequent in maritime precipitation. The rain attenuation is also found to be higher for maritime rain than continental rain and the difference increases with increase in rain intensity. The results will be useful for improvement of QPE and identification of the origin of different rain types from radar remote sensing observations.

Acknowledgement

Authors thankfully acknowledge the financial support provided by the Department of Science and Technology, Govt. of India (DST/INSPIRE/04/2014/002492) under INSPIRE Faculty Scheme. Authors also acknowledge the SAC, ISRO for the contribution in data collections.

References

Adler Jr., R.F., Wang, J.-J., Gu, G., Huffman, G., 2009. A ten-year tropical rainfall climatology based on a composite of TRMM products. J. Meteorol. Soc. Jpn. 87, 281–293.
Asen, W., Gibbins, C.J., 2002. A comparison of rain attenuation and drop size distributions measured in Chilbolton and Singapore. Radio Sci. 37, 1–15.
Atlas, D., Ulbrich, C.W., 1977. Path- and area-integrated rainfall measurement by microwave attenuation in the 1-3 cm Band. J. Appl. Meteorol. 16, 1322–1331.
Bringi, V.N., Chandrasekar, V., 2001. Polarimetric Doppler Weather Radar: Principles and Applications. Cambridge University Press, Cambridge.
Bringi, V.N., Chandrasekar, V., Hubbert, J., Gorgucci, E., Randeu, W.L., Schoenhuber, M., 2003. Raindrop size distribution in different climatic regimes from disdrometer and dual-polarized radar analysis. J. Atmos. Sci. 60, 354–365.
Chandra, N., Venkataramani, S., Lal, S., Sheel, V., Pozzer, A., 2016. Effects of convection and long-range transport on the distribution of carbon monoxide in the troposphere over India. Atmos. Pollut. Res. 7, 775–785.
Das, S., Ghosh, D., 2016. Dependency of rain integral parameters on specific rain drop sizes and its seasonal behaviour. J. Atmos. Sol. Terr. Phys. 149, 15–20.
Das, S., Maitra, A., 2016. Vertical profile of rain: Ka band radar observations at tropical locations. J. Hydrol. 534, 31–41.
Das, S., Maitra, A., 2017. Characterization of tropical precipitation using drop size distribution and rain rate-radar reflectivity relation. Theor. Appl. Climatol. 1–12. https://doi.org/10.1007/s00704-017-2073-1 (in press).
Das, S., Maitra, A., Shukla, A., 2010. Rain attenuation modelling in the 10–100GHz frequency using drop size distributions for different climatic zones in tropical India. Prog. Electromagn. Res. B 25, 211–224.
Delgado, G., Machado, L.A.T., Angelis, C.F., Bottino, M.J., Redaño, Á., Lorente, J., Gimeno, L., Nieto, R., 2008. Basis for a rainfall estimation technique using IR-VIS cloud classification and parameters over the life cycle of mesoscale convective systems. J. Appl. Meteorol. Climatol. 47, 1500–1517.
Deshpande, R.D., Dave, M., Padhya, V., Kumar, H., Gupta, S.K., 2015. Water vapour source identification for daily rain events at Ahmedabad in semi-arid western India: wind trajectory analyses. Meteorol. Appl. 22, 754–762.
Doviak, R.J., Zrnić, D.S., 1984. Doppler Radar and Weather Observations. Academic Press, Orlando, Fla, pp. 184–194.
Draxler, R.R., Hess, G.D., 1998. An overview of the HYSPLIT_4 modelling system for trajectories, dispersion, and deposition. Aust. Meteorol. Mag. 47, 295–308.
Feingold, G., Levin, Z., 1986. The lognormal fit to raindrop spectra from frontal convective clouds in Israel. J. Clim. Appl. Meterol. 25, 1346–1363.
Göke, S., Ochs III, H.T., Rauber, R.M., 2007. Radar analysis of precipitation initiation in maritime versus continental clouds near the Florida coast: inferences concerning the role of CCN and Giant Nuclei. J. Atmos. Sci. 64, 3695–3707.
Gunn, R., Kinzer, G.D., 1949. The terminal velocity of fall for water droplets in stagnant air. J. Meteorol. 6, 243–248.
Harikumar, R., Sampath, S., Sasi Kumar, V., 2010. Variation of rain drop size distribution with rain rate at a few coastal and high altitude stations in southern peninsular India. Adv. Space Res. 45, 576–586.
International Telecommunication Union, 2005. Specific Attenuation Model for Rain for Use in Prediction Methods. Recommendation ITU-R, P.838-3, Geneva.
Ippolito, L.J., 1986. Radio Wave Propagation in Satellite Communications, first ed. Van Nostrand Reinhold Company, New York.
Islam, T., Rico-Ramirez, M.A., Han, D., Srivastava, P.K., Ishak, A.M., 2012a. Performance evaluation of the TRMM precipitation estimation using ground-based radars from the GPM validation network. J. Atmos. Sol. Terr. Phys. 77, 194–208.
Islam, T., Rico-Ramirez, M.A., Han, D., Srivastava, P.K., 2012b. Joss–Waldvogel disdrometer derived rainfall estimation study by collocated tipping bucket and rapid response rain gauges. Atmos. Sci. Lett. 13, 139–150. https://doi.org/10.1002/asl.376.
Janapati, J., Seela, B.K., Reddy, M.V., Reddy, K.K., Lin, P.L., Rao, T.N., Liu, C.Y., 2017. A study on raindrop size distribution variability in before and after landfall precipitations of tropical cyclones observed over southern India. J. Atmos. Sol. Terr. Phys. 159, 23–40. https://doi.org/10.1016/j.jastp.2017.04.011.
Joss, J., Waldvogel, A., 1969. Raindrop size distribution and sampling size errors. J. Atmos. Sci. 16, 112–113.
Kirankumar, N.V.P., Rao, T.N., Radhakrishna, B., Rao, D.N., 2008. Statistical characteristics of raindrop size distribution in southwest monsoon season. J. Appl. Meteorol. Climatol. 47, 576–590.
Kozu, T., Nakamura, K., 1991. Rainfall parameter estimation from dual-radar measurements combining reflectivity profile and path-integrated attenuation. J. Atmos. Ocean. Technol. 8, 259–270.
Kozu, T., Reddy, K.K., Mori, S., Thurai, M., Ong, J.T., Rao, D.N., 2006. Seasonal and diurnal variations of raindrop size distribution in Asian monsoon region. J. Meteor. Soc. Japan 84A, 195–209.
Kumar, L.S., Lee, Y.H., Yeo, J.X., Ong, J.T., Kumar, L.S., 2011. Tropical rain classification and estimation of rain from Z-R (Reflectivity-rain Rate) relationships. Prog. Electromagn. Res. B 32, 107–127.
Lee, G.W., Zawadzki, I., 2005. Variability of drop size distributions: time-scale dependence of the variability and its effects on rain estimation. J. Appl. Meteorol. 44, 241–255.
Maitra, A., Das, S., Shukla, A.K., 2009. Joint statistics of rain rate and event duration for a tropical location in India. Indian J. Radio Space Phys. 38, 353–360.
McFarquhar, G.M., List, R., Hudak, D.R., Nissen, R.P., Dobbie, J.S., Tung, N.P., Kang, T.S., 1996. Flux measurements of pulsating rain with a disdrometer and Doppler radar during phase II of the joint tropical rain experiment in Malaysia. Appl. Meteor. 35, 859–874.
Montopoli, M., Roberto, N., Adirosi, E., Gorgucci, E., Baldini, L., 2017. Investigation of weather radar quantitative precipitation estimation methodologies in complex orography. Atmosphere (Basel) 8, 34.
Morin, E., Gabella, M., 2007. Radar-based quantitative precipitation estimation over mediterranean and dry climate regimes. J. Geophys. Res. Atmos. 112, 1–13.
Moupfouma, F., 1984. Improvement of a rain attenuation prediction method for terrestrial microwave links. IEEE Trans. Antenn. Propag. 32, 1368–1372.
Nesbitt, S.W., Cifelli, R., Rutledge, S. a., 2006. Storm morphology and rainfall characteristics of TRMM precipitation features. Mon. Weather Rev. 134, 2702–2721.
Ojo, J.S., Omotosho, T.V., 2013. Comparison of 1-min rain rate derived from TRMM satellite data and raingauge data for microwave applications in Nigeria. J. Atmos. Sol. Terr. Phys. 102, 17–25.
Purdie, H., Bertler, N., Mackintosh, A., Baker, J., Rhodes, R., 2010. Isotopic and elemental changes in winter snow accumulation on glaciers in the Southern Alps of New Zealand. J. Clim. 23, 4737–4749.
Raghavan, S., 2013. Radar Meteorology, Atmospheric and Oceanographic Sciences Library. Springer, Netherlands, pp. 267–169.
Rao, T.N., Rao, D.N., Mohan, K., Raghavan, S., 2001. Classification of tropical precipitating systems and associated Z–R relationships. J. Geophys. Res. 106, 1769917 711.
Rao, T.N., Radhakrishna, B., Nakamura, K., Rao, N.P., 2009. Notes and correspondence differences in raindrop size distribution from southwest monsoon to northeast monsoon at Gadanki. Q. J. R. Meteorol. Soc. 135, 1630–1637.
Rosenfeld, D., Lensky, I.M., 1998. Satellite-based insights into precipitation formation processes in continental and maritime convective clouds. Bull. Am. Meteorol. Soc. 79, 2457–2476.
Rosenfeld, D., Ulbrich, C.W., 2003. Cloud microphysical properties, processes, and rainfall estimation opportunities. Radar and Atmospheric Science: a collection of essays in honor of David Atlas. Meteor. Monogr. Amer. Meteor. Soc. 52, 237–258.
Sarkar, T., Das, S., Maitra, A., 2015. Assessment of different raindrop size measuring techniques: Inter-comparison of Doppler radar, impact and optical disdrometer. Atmos. Res. 160, 15–27. https://doi.org/10.1016/j.atmosres.2015.03.001.
Sauvageot, H., Lacaux, J.-P., 1995. The shape of averaged drop size distributions. J. Atmos. Sci. 52, 1070–1083.
Tapiador, F.J., Checa, R., De Castro, M., 2010. An experiment to measure the spatial variability of rain drop size distribution using sixteen laser disdrometers. Geophys. Res. Lett. 37, 1–6.
Tenório, R.S., Moraes, M. Cristina da Silva, Sauvageot, H., 2012. Raindrop size distribution and radar parameters in coastal tropical rain systems of northeastern Brazil. J. Appl. Meteorol. Climatol. 51, 1960–1970.
Thurai, M., Gatlin, P.N., Bringi, V.N., 2016. Separating stratiform and convective rain types based on the drop size distribution characteristics using 2D video disdrometer data. Atmos. Res. 169, 416–423.

Tian, Y., Peters-Lidard, C.D., Choudhury, B.J., Garcia, M., 2007. Multitemporal analysis of TRMM-based satellite precipitation products for land data assimilation applications. J. Hydrometeorol. 8, 1165–1183.

Timothy, K.I., Jin, Teong Ong, Choo, E.B.L., 2002. Raindrop size distribution using method of moments for terrestrial and satellite communication applications in Singapore. IEEE Trans. Antenn. Propag. 50, 1420–1424.

Tokay, A., Kruger, A., Krajewski, W.F., Kucera, P.A., Filho, A.J.P., 2002. Measurements of drop size distribution in the southwestern Amazon basin. J. Geophys. Res. 107 (D20), 8052. https://doi.org/10.1029/2001JD000355.

Ulbrich, C.W., 1983. Natural variations in the analytical form of the raindrop size distribution. J. Clim. Appl. Meteorol. 22, 1764–1775.

Ulbrich, C.W., Atlas, D., 2007. Microphysics of raindrop size spectra: tropical continental and maritime storms. J. Appl. Meteorol. Climatol. 46, 1777–1791.

Ulbrich, C.W., Lee, L.G., 1999. Rainfall measurement error by WSR-88D radars due to variations in Z-R law parameters and the radar constant. J. Atmos. Ocean. Technol. 16 (8), 1017–1024.

van De Beek, C.Z., Leijnse, H., Hazenberg, P., Uijlenhoet, R., 2016. Close-range radar rainfall estimation and error analysis. Atmos. Meas. Tech. 9, 3837–3850.

Wang, Y.Q., Zhang, X.Y., Draxler, R.R., 2009. TrajStat: GIS-based software that uses various trajectory statistical analysis methods to identify potential sources from long-term air pollution measurement data. Environ. Model. Software 24, 938–939. https://doi.org/10.1016/j.envsoft.2009.01.004.

Wilson, J.W., Brandes, E. a., 1979. Radar measurement of rainfall—a summary. Bull. Am. Meteorol. Soc. 60, 1048–1058.

Yeo, T.S., Kooi, P.S., Leong, M.S., Li, L.W., 2001. Tropical raindrop size distribution for the prediction of rain attenuation of microwaves in the 10-40 GHz band. IEEE Trans. Antenn. Propag. 49, 80–83.

Yum, Seong Soo, Hudson, James G., 2002. Maritime/continental microphysical contrasts in stratus. Tellus B 54, 61–73.

Zipser, E.J., Cecil, D.J., Liu, C., Nesbitt, S.W., Yorty, D.P., 2006. Where are the most: intense thunderstorms on Earth? Bull. Am. Meteorol. Soc. 87, 1057–1071.